pISSN 1229-845X, eISSN 1976-555X
J. Vet. Sci. (2014), **15**(1), 51-60
http://dx.doi.org/10.4142/jvs.2014.15.1.51
Received: 24 Jun. 2013, Revised: 4 Sep. 2013, Accepted: 6 Oct. 2013

JOURNAL OF
Veterinary
Science

Original Article

Protective effects of silymarin on fumonisin B_1-induced hepatotoxicity in mice

Mahmut Sozmen[1,*], Alparslan Kadir Devrim[2], Recai Tunca[3], Murat Bayezit[4], Serpil Dag[5], Dinc Essiz[6]

[1]*Department of Pathology, Samsun, Faculty of Veterinary Medicine, University of Ondokuz Mayis, Samsun 55139, Turkey*
Departments of [2]Biochemistry and [4]Pharmacology and Toxicology, Faculty of Veterinary Medicine, University of Mehmet Akif Ersoy, Burdur 15100, Turkey
[3]*Department of Pathology, Faculty of Veterinary Medicine, University of Adnan Menderes, Aydin 09010, Turkey*
[5]*Department of Pathology, Faculty of Veterinary Medicine, University of Kafkas, Kars 36100, Turkey*
[6]*Department of Pharmacology and Toxicology, Faculty of Veterinary Medicine, University of Kirikkale, Kirikkale 71450, Turkey*

The present study was conducted to investigate the effect of silymarin on experimental liver toxication induced by Fumonisin B_1 (FB_1) in BALB/c mice. The mice were divided into six groups (n = 15). Group 1 served as the control. Group 2 was the silymarin control (100 mg/kg by gavage). Groups 3 and 4 were treated with FB_1 (Group 3, 1.5 mg/kg FB_1, intraperitoneally; and Group 4, 4.5 mg/kg FB_1). Group 5 received FB_1 (1.5 mg/kg) and silymarin (100 mg/kg), and Group 6 was given a higher dose of FB_1 (4.5 mg/kg FB_1) with silymarin (100 mg/kg). Silymarin treatment significantly decreased ($p < 0.0001$) the apoptotic rate. FB_1 administration significantly increased ($p < 0.0001$) proliferating cell nuclear antigen and Ki-67 expression. Furthermore, FB_1 elevated the levels of caspase-8 and tumor necrosis factor-alpha mediators while silymarin significantly reduced ($p < 0.0001$) the expression of these factors. Vascular endothelial growth factor (VEGF) and fibroblast growth factor-2 (FGF-2) expressions were significantly elevated in Group 4 ($p < 0.0001$). Silymarin administration alleviated increased VEGF and FGF-2 expression levels ($p < 0.0001$). In conclusion, silymarin ameliorated toxic liver damage caused by FB_1 in BALB/c mice.

Keywords: caspase-8, fumonisin B1, fibroblast growth factor-2, galectin-3, silymarin

Introduction

Fumonisins are mycotoxins produced mainly by *Fusarium* (*F.*) *verticillioides*, *F. moniliforme*, and *F. proliferatum*. These fungi are ubiquitous contaminants of corn, sorghum, and related grain products consumed throughout the world by both humans and animals [27]. Fumonisin B_1 (FB_1), the most toxic and abundant fumonisin, induces liver damage many animals [26].

Silymarin, a natural and potent polyphenolic flavonoid antioxidant extracted from milk thistle (*Silybum marianum*) can minimize damage by free radicals and while conferring protection against oxidative stress and toxicity [19]. Galectin-3 (Gal-3), a β-galactoside-binding animal lectin, plays a pivotal role in diverse functions such as cell growth, anti-apoptotic activity, and mRNA splicing [17]. Gal-3 is not expressed in normal mouse liver hepatocytes [14]. However, expression of this factor is induced in the cytoplasm of periportal hepatocytes injured by CCl_4. This indicates that Gal-3 is a novel signaling protein that acts downstream of tyrosine kinase, and can promote the repair or survival of injured hepatocytes rather than increase cell proliferation [28].

FB_1 administration in mice induces caspase-8 enzyme activity. Caspase-8 is an intracellular downstream signalling molecule involved in the tumor necrosis factor-alpha (TNFα) apoptotic pathway and plays a role in FB_1-induced apoptosis [5]. Silymarin inhibits the production of endogenous tumor promoter TNFα [30].

In the present study the effects of FB_1 and the ability of silymarin to protect against FB_1 toxicity, prevent apoptosis, and affect hepatocyte proliferation rates were evaluated. For this, the expression of proliferating cell nuclear antigen (PCNA) and Ki-67 was measured in female mice. The role of TNFα and its interaction with

*Corresponding author: Tel: +90-505-7717746; Fax: +90-362-4576922; E-mail: msozmen@hotmail.com

caspase-8 in cases of FB_1-induced hepatotoxicity *in vivo* was also explored in an experimental BALB/c mouse model. We also determined whether FB_1-induced hepatotoxicity can increase vascular endothelial growth factor (VEGF) and fibroblast growth factor-2 (FGF-2) expression, and consequently stimulate angiogenesis and fibrogenesis.

Materials and Methods

Animals and husbandry

The study design was approved by the experimental ethics committee of the University of Kafkas (Turkey). All animals were maintained in accordance with university policies. In this study, female mice were used because females show greater sensitivity to FB_1-induced hepatotoxicity compared to males [9]. Ninety BALB/c female mice (University of 19 Mayis, Faculty of Medicine, Turkey) 10 weeks old and weighing an average of 30 ± 1.93 g were divided into six groups (15 females per group kept in separate cages). The mice were housed in stainless-steel wire-mesh cages in a well-ventilated, temperature-controlled room (23 ± 2°C) with 55% relative humidity and a 12-h light/dark cycle. The animals had free access to laboratory rodent chow (Toros Feed, Turkey) and tap water up to the time of sacrifice.

Experimental design and treatment of animals

The mice were randomly divided into six groups (n = 15). Each group was further divided into three sub-groups (n = 5; A, B, and C). Only physiological saline (0.1 mL) was administered intraperitoneally (IP) every day to the control group (Group 1) for 14 days. The silymarin control group (Group 2) received only silymarin (CAS: 65666-01-1, S0292; Sigma-Aldrich, USA) by gavage (100 mg/kg) every day for 14 days. FB_1 (CAS: 116355-83-0; kindly provided by Dr. Ronald Riley; Toxicology and Mycotoxin Research Unit, United States Department of Agriculture-Agricultural Research Service, USA) was administered to Groups 3 (1.5 mg/kg FB_1, IP) and 4 (4.5 mg/kg FB_1, IP) every other day starting from Day 1 (for the details please see Table 1). For Groups 5 (1.5 mg/kg FB_1) and 6 (4.5 mg/kg FB_1), FB_1 was administered from day 1 for 14 days. Groups 5 and 6 also received silymarin (100 mg/kg, gavage) daily for 14 days starting from Day 0. Five mice from each group were sacrificed by cervical dislocation on Days 14, 17, and 21 (sub-groups A, B, and C, respectively; Table 1). The treatment protocol was based on previous studies showing that FB_1 induces liver injury in a dose-dependent manner [3,9].

Histopathological evaluation of liver tissues

Animals were euthanized by cervical dislocation. The liver was removed, weighed, cut into sections in 5 mm thickness with a surgical blade, and immediately fixed in 10% neutral buffered formalin. After fixation, the tissues were embedded in paraffin, cut into sections with a microtome (Leica RM2125RT; Leica, Germany) in 5 μm, and stained with hematoxylin and eosin (H&E; Hematoxylin crystals purchased from Merck, Germany; Eosin Y was purchased from Carlo Erba, Italy) for histological examination.

Immunohistochemistry

Sections from all tissue samples were cut into sections 5-μm thick and processed for immunohistochemical examination with a streptavidin-biotin-peroxidase method. The tissue sections were placed on slides (Isolab Laborgeräte, Germany) coated with 3-amino-propyltrieyhoxysilane (Sigma-Aldrich, USA), dewaxed, and hydrated by using decreasing dilutions

Table 1. Experimental design, groups and sub-groups, chemicals, dose, and treatment periods

Groups and sub-groups	Mice (n)	Chemical administered	Dose and administration route	Treatment days														Sampling days Mice (n)		
				0	1	2	3	4	5	6	7	8	9	10	11	12	13	14	17	21
1 A, B, C	15	PS	0.1 mL (IP)	-	PS	-	PS	-	PS	-	PS	-	PS	-	PS	-	PS	5	5	5
2 A, B, C	15	S	100 mg/kg (G)	S	S	S	S	S	S	S	S	S	S	S	S	S	S	5	5	5
3 A, B, C	15	FB_1	1.5 mg/kg (IP)	-	FB_1	-	FB_1	-	FB_1	-	FB_1	-	FB_1	-	FB_1	-	FB_1	5	5	5
4 A, B, C	15	FB_1	4.5 mg/kg (IP)	-	FB_1	-	FB_1	-	FB_1	-	FB_1	-	FB_1	-	FB_1	-	FB_1	5	5	5
5 A, B, C	15	FB_1 + S	1.5 mg/kg (IP) + 100 mg/kg (G)	S	FB_1 + S	S	FB_1 + S	S	FB_1 + S	S	FB_1 + S	S	FB_1 + S	S	FB_1 + S	S	FB_1 + S	5	5	5
6; A, B, C	15	FB_1 + S	4.5 mg/kg (IP) + 100 mg/kg (G)	S	FB_1 + S	S	FB_1 + S	S	FB_1 + S	S	FB_1 + S	S	FB_1 + S	S	FB_1 + S	S	FB_1 + S	5	5	5

PS: physiologic saline, S: silymarin, FB1: fumonisin B1, IP: intraperitoneal, G: gavage.

Table 2. Specificity and dilution factors of antibodies used

Specificity	Source and antibody dilution	
FGF-2	Rabbit pAb IgG, sc-79 (147); Santa Cruz Biotechnology, USA	1 : 100
Gal-3	Rabbit pAb IgG, H-160, sc-20157; Santa Cruz Biotechnology	1 : 100
VEGF	Mouse mAb IgG2a, C-1, sc-7269; Santa Cruz Biotechnology	1 : 100
Ki-67	Mouse mAb IgG1, MM1, Novocastra Reagents; Leica Biosystems, UK	1 : 100
PCNA	Mouse mAb IgG2a, PC10, Novocastra Reagents; Leica Biosystems	1 : 1000
Caspase-8	Rabbit pAb IgG, Flice, Ab-4; Thermo Fisher Scientific, USA	1 : 100
TNFα	Rabbit pAb IgG, HP8001; Hycult Biotech, The Netherlands	1 : 10

of ethanol from 100% to 50%. Antigen retrieval was performed by heating the sections in citrate buffer (pH 6.0) for 10 min in a microwave oven (M1733N; Samsung, Malaysia) at 800 watts. The slides were then dipped in freshly prepared absolute methanol containing 3% (v/v) hydrogen peroxide for 15 min at room temperature to block endogenous peroxidase activity. The slides were then incubated with polyclonal or monoclonal antibodies (Table 2) for 1 h at room temperature. Next, the sections were exposed to biotinylated goat anti-rabbit IgG (Dako, USA) or rabbit anti-mouse IgG (Dako) diluted 1 : 300 in phosphate-buffered saline (PBS) for 30 min at room temperature. The slides were subsequently incubated with streptavidin peroxidase complex (ABC; Dako) diluted 1 : 300 in Tris-buffered solution for 30 min at room temperature. After repeated washing with PBS, the sections were incubated with 3,3´-diaminobenzidine tetrahydrocholoride (DAB; Dako) in distilled water (0.5 mg DAB/mL) containing 30% (v/v) hydrogen peroxide for 2 min. and the reaction was halted by immersing sections in tap water at room temperature. Finally, the sections were counterstained with Mayer's hematoxylin (Merck), dehydrated, and mounted (Entellan; Merck). Negative control tissue sections were incubated with undiluted normal goat or rabbit serum (Dako, Denmark).

Terminal deoxynucleotidyl transferase (TdT)-mediated deoxyuridine-5´-triphosphate (dUTP)-biotin nick end labeling (TUNEL) assay for apoptotic cells

Apoptotic cells were detected using a DeadEnd TUNEL system (Promega, USA) according to the manufacturer's protocol with some modifications. In brief, deparaffinized and rehydrated tissue sections were permeabilized with proteinase K (20 μg/mL; Promega) for 30 min at room temperature. After thoroughly washing with 3× PBS, the sections were incubated with equilibration buffer for 10 min. Next, 100 μL of terminal deoxynucleotidyl transferase reaction mixture was added to the sections except for the negative control and incubated at 37°C for 1 h. The reaction was stopped by immersing the sections in 2× saline-sodium citrate buffer at room temperature for 15 min. Endogenous peroxidase activity was then quenched by incubation in 0.3% hydrogen peroxide at room temperature for 10 min. The sections were subsequently treated with horseradish peroxidase-conjugated streptavidin (1 : 500) for 30 min at room temperature. After repeated washing with PBS, the tissue samples were incubated with 3,3´-diaminobenzidine (Promega) in distilled water (0.5 mg DAB/mL) containing 30% (v/v) hydrogen peroxide and the reaction was halted by immersing sections in tap water at room temperature. Finally, the sections were counterstained with Harris hematoxylin (Merck), or methylene blue (Merck). The sections, then, were dehydrated by using increasing percentages of alcohol from 50% to 100% and cleared with xylene (Merck) and mounted (Entellan; Merck) before being examined at 400× magnification (Nikon Eclipse E600; Nikon, Japan) for TUNEL-positive cells.

Analysis of Gal-3, caspase-8, TNFα, FGF-2, and VEGF immunostaining

Cells positive for Gal-3 and caspase-8 were semi-quantitatively assessed with a light microscope (Nikon Eclipse E600; Nikon). For immunostaining quantification, an area with the highest density of positive cells was chosen. To calculate the total number of positively stained cells, an ocular grid of 100 (10 × 10) squares was used at 400× magnification. Cells in a total of ten high-power fields (0.025 mm^2) were counted. The percentages of positive versus negative cells were recorded in the ten fields and the mean value was the final score. The analyses of TNFα, FGF-2, and VEGF immunostaining were slightly different because staining intensities significantly differed between the sub-groups of every group. For this reason, percentages of positively stained cells were multiplied by cytoplasmic staining intensity scores: (1) weak, (2) moderate, and (3) intense.

Analysis of Ki-67, PCNA, mitosis, and TUNEL assay findings

Results of the Ki-67, PCNA, mitosis, and TUNEL assays were assessed using a grading system based on the total number of positive cells. The mitotic rate was calculated by

counting the number of mitotic figures. All positive cells for the TUNEL assay as well as Ki-67 and PCNA staining or mitotic figures were counted among approximately 1,400 cells per sample from a total of 10 high-power fields (0.025 mm^2). To calculate the total number of positively stained cells, an ocular grid of 100 (10 × 10) squares was used at 400× magnification. The intensity of Ki-67 and PCNA staining in the cytoplasm and nucleus was assessed semi-quantitatively based on the following scale: (0) none, (1) weak, (2) moderate, or (3) intense.

Statistical analyses

Differences between the groups were tested with a one-way analysis of variance (ANOVA) and Tukey's test using statistical package for the social sciences for Windows version 10.0 (SPSS, USA). Data are presented as the mean ± standard error (SE). A p values less than 0.05 were considered significant.

Results

Histopathological findings

Histopathological examination revealed that livers from the control and silymarin groups were normal in appearance with typical histological structures. FB_1 treatment (Group 3; 1.5 mg/kg FB_1) caused degenerative changes in the hepatocytes including mild vacuolar degeneration, bile duct hyperplasia, megalocytosis (Fig. 1A), and mitosis (Fig. 1B). Severity of the lesions was similar among sub-groups 3A, 3B, and 3C. The degenerative changes were more severe in mice treated with 4.5 mg/kg FB_1. Silymarin administration alleviated lesion severity in both Groups 5 and 6. However, the occasional presence of apoptotic figures (Fig. 1C) and spherical, eosinophilic intranuclear inclusion bodies formed by invagination of the cytoplasm into nucleus persisted in all groups (Fig. 1D).

Detection of apoptotic cells using a TUNEL assay and mitosis evaluation

Apoptotic cells were identified in all the cases by the TUNEL assay. Three different patterns of TUNEL-positive reactions were observed either alone or in combination: brown products in both non-pyknotic nuclei and cytoplasm (Fig. 1E), cytoplasmic staining alone (Fig. 1F), and appearance of non-identifiable rounded or irregular structures (so-called "apoptotic bodies") either free among the hepatocytes or within the cytoplasm (Fig. 1G). TUNEL-positive signals were also observed among necrotic debris along with some Kupffer and other inflammatory cells. In the negative tissue section control, substitution of the TUNEL reaction mixture with labeling solution lacking terminal transferase produced negative results.

TUNEL-positive signals (Table 3) were occasionally observed in the control (Group 1) and mice treated with silymarin alone (Group 2). FB_1 administration caused a statistically significant increase in apoptotic bodies in Groups 3 and 4 ($p < 0.0001$). Silymarin treatment significantly ameliorated the deleterious effects of FB_1, particularly in Group 5 animals ($p < 0.0001$).

Mitotic figures (Table 3) were occasionally observed in the control (Group 1) and animals treated with silymarin

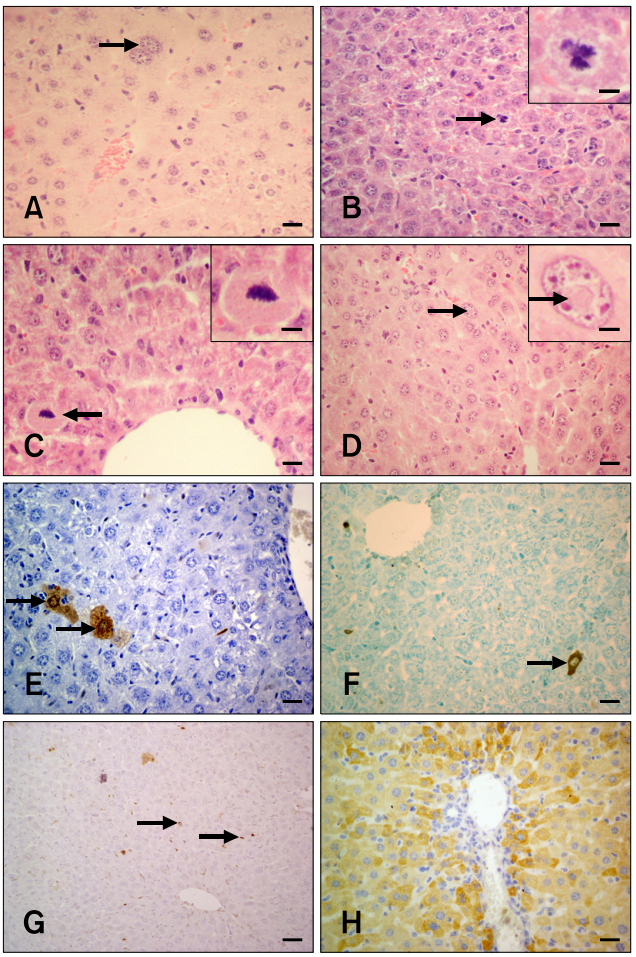

Fig. 1. H&E, TUNEL, and caspase-8-specific immunohistochemistry in hepatocytes from the experimental and control groups. (A) Megalocytosis in mouse liver (arrow; Group 1A). (B) Mitosis in mouse hepatocytes (arrow; Group 3A). (C) An apoptotic hepatocyte with a pycnotic nucleus (arrow; Group 5A). (D) Eosinophilic, intranuclear inclusion body in a mouse hepatocyte (arrow; Group 6A). (E) Cytoplasm and nucleus of two non-pyknotic hepatocytes exhibiting a TUNEL-positive reaction (arrows; Group 3A). (F) Cytoplasmic reaction in mouse liver. The non-pyknotic nucleus is negative (arrow; Group 6A). (G) Free apoptotic bodies in the liver parenchyma (arrows; Group 5A). (H) Hepatocytes exhibiting cytoplasmic staining for caspase-8 (Group 3B). H&E staining (A ~ D), TUNEL assay results (E ~ G), Harris hematoxylin counterstaining (E), methylene blue counterstaining (F), and Mayer's hematoxylin counterstain (G). Scale bars = 6 μm (B inset and D inset), 8.5 μm (C inset), 13 μm (A), 17 μm (C), 22 μm (B, D ~ F, and H), and 44 μm (G).

Table 3. Caspase-8, Ki-67, PCNA, TNFα, FGF-2, VEGF, mitotic count, and TUNEL assay analysis results for the main groups

Groups	Mitosis	Apoptosis	Caspase-8	Ki-67	Gal-3	PCNA	TNFα	FGF-2	VEGF
1	0.08 ± 0.3	0.33 ± 0.49	0.00 ± 0.00	0.17 ± 0.58	0.00 ± 0.00	0.74 ± 0.24	45.00 ± 0.00	35.83 ± 11.25	1.25 ± 1.06
	B	C	B	C		B	C	BC	B
2	0.11 ± 0.3	0.67 ± 0.50	0.00 ± 0.00	0.22 ± 0.67	0.00 ± 0.00	0.94 ± 0.15	63.33 ± 7.91	38.56 ± 7.30	2.11 ± 2.76
	B	C	B	C		B	BC	BC	B
3	1.59 ± 2.8	13.71 ± 5.36	50.29 ± 37.68	103.47 ± 94.04	1.41 ± 2.27	8.75 ± 8.54	141.24 ± 42.65	34.88 ± 26.18	22.00 ± 26.28
	A	A	A	BC		A	A	BC	B
4	0.50 ± 0.9	11.43 ± 5.05	38.21 ± 26.72	268.43 ± 252.39	1.61 ± 2.54	9.64 ± 7.10	124.57 ± 33.55	82.86 ± 33.44	49.68 ± 52.34
	AB	A	A	A		A	A	A	A
5	0.20 ± 04	7.33 ± 5.89	14.60 ± 25.62	187.53 ± 159.78	0.80 ± 2.57	8.56 ± 6.37	115.60 ± 60.43	52.33 ± 16.57	12.93 ± 11.05
	B	B	B	AB		A	A	B	B
6	0.64 ± 0.8	10.91 ± 6.09	11.73 ± 11.68	260.27 ± 256.20	0.55 ± 1.51	8.23 ± 5.17	80.82 ± 27.01	26.18 ± 25.49	10.19 ± 8.63
	AB	AB	B	A		A	B	C	B
p-value	0.042	0.000	0.000	0.000	NS	0.000	0.000	0.000	0.000

Values are presented as the mean ± SE. A, B, and C: Mean values with different letters in the same column indicate statistically significant differences. NS: not significant.

alone (Group 2). FB_1 administration caused a significant increase of mitotic figures in Group 3 animals. Silymarin treatment significantly decreased mitotic figure formation in Group 5 ($p < 0.05$).

Immunohistochemistry

Immunohistochemical examinations revealed that FB_1 administration caused a statistically significant increase of caspase-8, Ki-67, PCNA, and TNFα levels in the liver compared to the control and mice treated with silymarin alone. Semi-quantitative assessment of the immunostaning results and statistical differences among all groups and sub-groups are summarized in Tables 3 and 4.

Caspase-8

Immunohistochemistry revealed marked cytoplasmic immunoreactivity of the hepatocytes (Fig. 1H) from mice that received FB_1 alone (Groups 3 and 4). However, the staining intensity was significantly decreased in silymarin-treated Groups 5 and 6 (Fig. 2A) compared to that observed mice receiving FB_1 alone ($p < 0.0001$).

Ki-67

Three different patterns of Ki-67-specific staining were observed in the liver tissue either alone or in combination: (1) brown products in both the nucleus and cytoplasm (Fig. 2B), (2) brown product only in the cytoplasm with a negative nucleus (Fig. 2B), and (3) nuclear staining alone (Fig. 2C). The reactions were diffuse with periacinar preponderance (Fig. 2C). The groups treated with silymarin alone showed very limited reaction while staining specific for Ki-67 was not observed for the control group. In contrast, FB_1 administration caused a significant increase in Ki-67-positive staining, particularly in Group 4 (Fig. 2D). The differences between groups treated with FB_1 and silymarin were not statistically significant although a significant decrease was observed in Group 6 on day 21 (Group 6C, $p < 0.005$; Fig. 2E).

Gal-3

With the exception of some Kupffer cells, staining for the Gal-3 antibody was not observed in the control or silymarin-treated groups. FB_1 administration caused a mild elevation of Gal-3 staining in both Groups 3 and 4 (Fig. 2F). Prominent Gal-3-specific reactions were also detected in Kupffer cells, neutrophils, and macrophages (Fig. 2G). Silymarin treatment alleviated the effects of FB_1 in Groups 5 (Fig. 2H) and 6. The decrease was more pronounced on day 21 (Groups 5C and 6C, Table 4).

PCNA

Three different patterns of PCNA-specific staining were observed in the liver tissue either alone or in combination: (1) both cytoplasmic and nuclear staining (Fig. 3A), (2) cytoplasmic staining alone with a negative nucleus (Fig. 3A), and (3) nuclear staining alone (Fig. 3A). Diffuse cytoplasmic or nuclear staining in the hepatocytes was mainly seen in the periacinar region (Fig. 3B). Expression levels for PCNA in the control and silymarin-treated groups were insignificant. On the other hand, FB_1 administration caused significant elevation of PCNA expression in Groups 3 and 4. The staining intensity was quite high on the 14th day in these two groups (Fig. 3C). PCNA levels decreased continuously and were at a minimal level on Day 21 in Groups 3 and 4. A combination of FB_1 and silymarin administration (Group 5) caused a significant decrease of

Table 4. Caspase-8, Ki-67, PCNA, TNFα, FGF-2, VEGF, mitotic count, and TUNEL assay analysis results for the sub-groups

Groups	Sub groups	Mitosis	Apoptosis	Caspase-8	Ki-67	Gal-3	PCNA	TNFα	FGF-2	VEGF
1	1A	0.00 ± 0.0	0.50 ± 0.58	0.00 ± 0.00	0.00 ± 0.00	0.00 ± 0.00	0.80 ± 0.16	45.00 ± 0.00	36.25 ± 16.01	0.25 ± 0.50
		B	C	B	B		C	B	B	B
2	2A	0.00 ± 0.0	0.67 ± 0.58	0.00 ± 0.00	0.67 ± 1.15	0.00 ± 0.00	1.00 ± 0.17	60.00 ± 13.23	40.00 ± 5.00	0.33 ± 0.58
		B	C	B	B		C	BC	B	B
3	3A	5.40 ± 2.2	10.40 ± 2.70	9.40 ± 11.59	130.20 ± 73.43	2.60 ± 3.29	17.42 ± 8.86	122.00 ± 38.83	42.00 ± 38.83	31.20 ± 33.12
		A	B	AB	B		A	A	B	AB
4	4A	0.80 ± 1.3	11.40 ± 4.04	22.00 ± 17.18	184.60 ± 138.73	3.30 ± 3.87	13.76 ± 5.34	92.80 ± 7.53	87.00 ± 19.24	57.50 ± 58.36
		B	AB	A	B		AB	AB	A	A
5	5A	0.40 ± 0.5	13.40 ± 6.15	2.60 ± 0.89	98.40 ± 82.35	2.40 ± 4.28	6.20 ± 6.78	104.80 ± 39.72	40.00 ± 0.00	18.60 ± 15.74
		B	AB	B	B		BC	A	B	AB
6	6A	1.50 ± 0.6	16.50 ± 3.87	3.25 ± 1.71	500.50 ± 257.21	1.25 ± 2.50	10.65 ± 4.95	100.00 ± 8.16	52.50 ± 25.00	9.50 ± 3.32
		B	A	B	A		AB	A	B	AB
p		0.000	0.000	0.014	0.000	NS*	0.002	0.003	0.021	0.089
1	1B	0.25 ± 0.5	0.25 ± 0.50	0.00 ± 0.00	0.00 ± 0.00	0.00 ± 0.00	0.53 ± 0.29	45.00 ± 0.00	35.00 ± 12.91	1.25 ± 0.96
			B	C	B	B	B	E	BC	
2	2 B	0.33 ± 0.6	0.67 ± 0.58	0.00 ± 0.00	0.00 ± 0.00	0.00 ± 0.00	0.90 ± 0.10	65.00 ± 5.00	40.00 ± 10.00	4.00 ± 4.00
			B	C	B	B	B	DE	BC	
3	3 B	0.00 ± 0.0	19.40 ± 6.07	39.60 ± 28.52	197.00 ± 68.40	2.20 ± 1.92	10.66 ± 3.76	138.20 ± 57.15	26.40 ± 10.83	25.20 ± 31.55
			A	AB	AB	A	A	BC	CD	
4	4 B	0.60 ± 0.9	11.40 ± 4.04	59.00 ± 32.48	304.20 ± 274.54	0.80 ± 0.45	12.55 ± 4.99	160.00 ± 18.71	93.00 ± 16.43	28.40 ± 10.26
			A	A	A	AB	A	AB	A	
5	5 B	0.20 ± 0.4	3.60 ± 2.41	17.60 ± 19.91	157.00 ± 166.76	0.00 ± 0.00	13.06 ± 6.09	180.00 ± 15.81	53.00 ± 16.43	13.40 ± 9.10
			B	BC	AB	B	A	A	B	
6	6 B	0.33 ± 0.6	11.67 ± 4.51	18.67 ± 15.50	236.67 ± 107.74	0.33 ± 0.58	6.93 ± 6.13	100.00 ± 0.00	6.00 ± 4.00	10.50 ± 14.72
			A	BC	AB	AB	AB	CD	D	
p		NS	0.000	0.006	0.064	0.049	0.003	0.000	0.000	NS
1	1C	0.00 ± 0.0	0.25 ± 0.50	0.00 ± 0.00	0.50 ± 1.00	0.00 ± 0.00	0.90 ± 0.08	45.00 ± 0.00	36.25 ± 6.29	2.25 ± 0.50
			B	C	B	B	B	B		B
2	2C	0.00 ± 0.0	0.67 ± 0.58	0.00 ± 0.00	0.00 ± 0.00	0.00 ± 0.00	0.93 ± 0.21	65.00 ± 5.00	35.67 ± 8.33	2.00 ± 2.00
			B	C	B	B	B	B		B
3	3C	0.00 ± 0.0	12.00 ± 2.77	87.14 ± 9.06	17.57 ± 19.33	0.00 ± 0.00	1.20 ± 0.75	157.14 ± 32.51	35.86 ± 25.33	13.14 ± 16.64
			A	A	B	B	B	A		B
4	4C	0.00 ± 0.0	11.50 ± 8.19	32.50 ± 9.57	328.50 ± 362.25	0.50 ± 0.58	0.85 ± 1.30	120.00 ± 23.09	65.00 ± 58.02	66.50 ± 77.17
			A	B	A	A	B	A		A
5	5C	0.00 ± 0.0	5.00 ± 2.74	23.60 ± 40.09	307.20 ± 160.51	0.00 ± 0.00	6.42 ± 4.57	62.00 ± 45.08	64.00 ± 18.17	6.80 ± 3.03
			B	BC	A	B	A	B		B
6	6C	0.00 ± 0.0	4.75 ± 1.50	15.00 ± 11.55	37.75 ± 37.03	0.00 ± 0.00	6.78 ± 5.21	47.25 ± 2.06	15.00 ± 5.77	10.65 ± 9.57
			B	BC	B	B	A	B		B
p		NS	0.000	0.000	0.006	0.017	0.006	0.000	NS	0.058

Values are presented as the mean ± SE. A, B, C, and D: Mean values marked with different letters in the same column indicate statistically significant differences. NS: not significant.

PCNA expression on the 14th day (Group 5A; Fig. 3D). However, this decrease was not constant and PCNA levels started to increase on Day 17 (Group 5B) and returned to the base level on Day 21 (Group 5C).

TNFα

TNFα-positive cytoplasmic staining was found in hepatocytes from all groups (Fig. 3E). Weak TNFα staining was observed in the control and silymarin-treated control groups. Liver sections from FB_1-exposed mice in Groups 3 and 4 exhibited a significant increase of TNFα expression

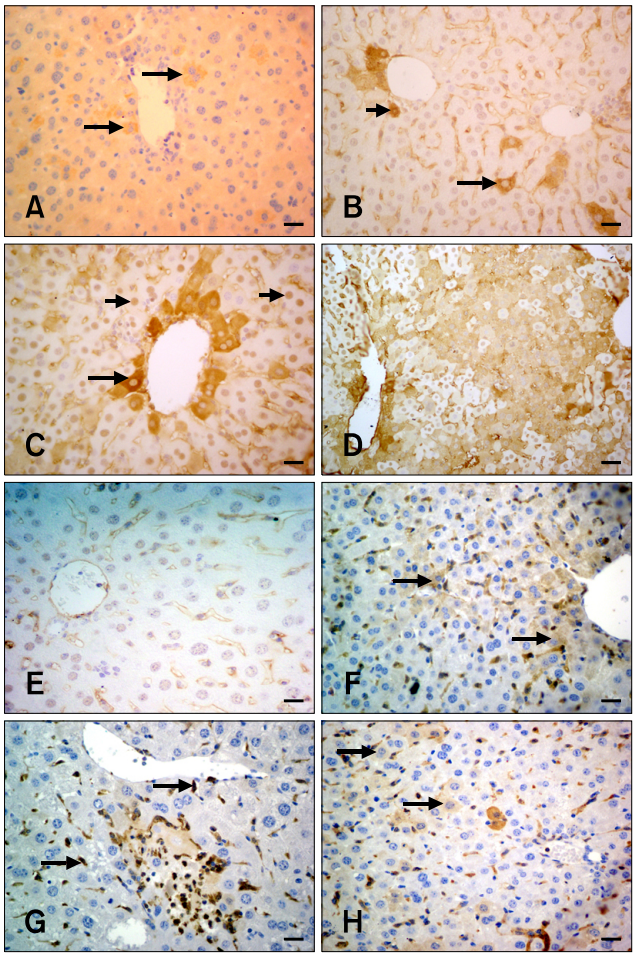

Fig. 2. Caspase-8, Ki-67, and Gal-3 immunohistochemistry in hepatocytes from the experimental and control groups. (A) Caspase-8 expression was observed in some periacinar hepatocytes (arrows; Group 6A). (B) In this panel, only the cytoplasm (long arrow) or both cytoplasm and nucleus (short arrow) are positive for Ki-67 (Group 5C). (C) Only the nucleus was positive for Ki-67 (short arrows). Periacinar hepatocyte cytoplasms were distinctively positive (long arrow) for Ki-67 expression (Group 3A). (D) Diffuse Ki-67-specific staining in mouse liver (Group 4B). (E) Hepatocytes were negative for the Ki-67 on the 21st day (Group 6C). (F) Weak cytoplasmic staining specific for Gal-3 in mouse liver (arrows; Group 3A). (G) Kupffer cells were intensely stained with the Gal-3 antibody (arrows). The hepatocytes were negative (Group 3A). (H) A limited number of hepatocytes showed weak cytoplasmic staining for the Gal-3 antibody (arrows; Group 5A). Scale bars = 15 μm (E), 22 μm (A ~ C and F ~ H), and 44 μm (D).

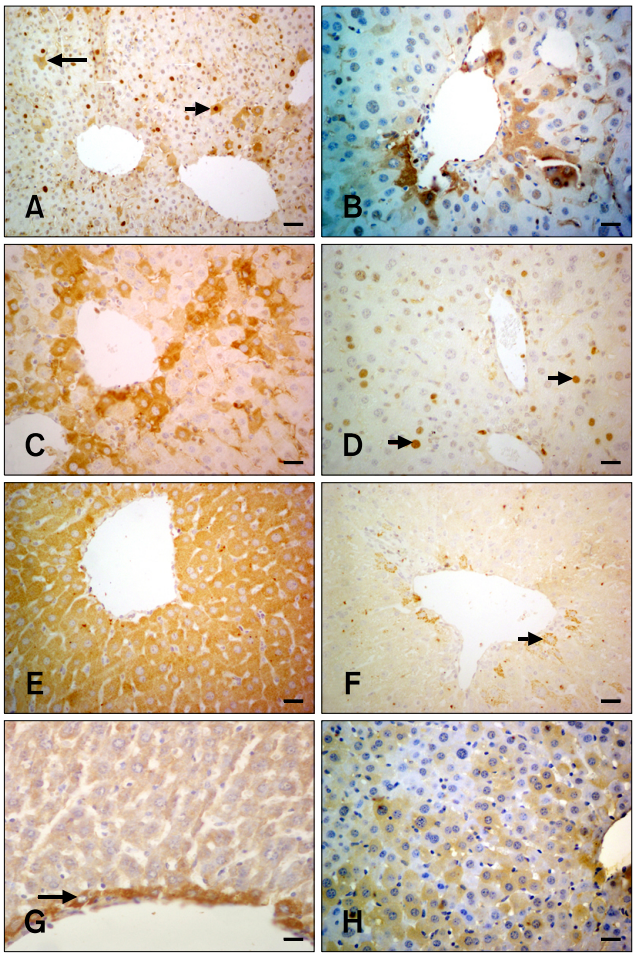

Fig. 3. PCNA, TNFα, and FGF-2 immunohistochemistry in hepatocytes from the experimental and control groups. (A) Only the nuclei are positive for PCNA (white arrows). Only cytoplasmic PCNA staining was observed in some hepatocytes while the nucleus was negative (long black arrow). Both cytoplasmic and nuclear staining with the PCNA antibody (short black arrow; Group 6B) is shown. (B) Cytoplasmic PCNA-specific staining in periacinar hepatocytes (Group 4B). (C) Intense cytoplasmic PCNA staining of the periacinar hepatocytes on the 14th day (Group 4A). (D) Decreased PCNA expression in the hepatocytes (arrows; Group 5A). (E) Diffuse cytoplasmic staining specific for TNFα; the nucleus is negative (Group 3C). (F) Cytoplasmic TNFα-specific staining of some periacinar hepatocytes (arrow; Group 5C). (G) Hepatocytes surrounding the central vein were positive for FGF-2 (arrow; Group 1A). (H) Cytoplasmic FGF-2 expression (Group 4A). Scale bars = 18 μm (G), 22 μm (B ~ F and H), and 44 μm (A).

($p < 0.0001$). Silymarin application significantly alleviated the effects of FB_1 in only Group 6 ($p < 0.0001$). High TNFα levels were significantly decreased on Day 21 in both Groups 5C (Fig. 3F) and 6C ($p < 0.0001$).

FGF-2

Cytoplasmic FGF-2 reactivity was mainly seen in hepatocytes surrounding the central vein. Other hepatocytes were negative in the control (Fig. 3G) and silymarin-treated control groups. The expression levels did not change in the group treated with 1.5 mg/kg FB_1 (Group 3). Increased dosage of FB_1 (4.5 mg/kg) significantly elevated the FGF-2 expression level in Group 4 (Fig. 3H). Silymarin treatment resulted in a significant decrease ($p < 0.0001$) of FGF-positive hepatocytes in Group 6. FGF reaction was only seen in the intralobular cells in Group 6.

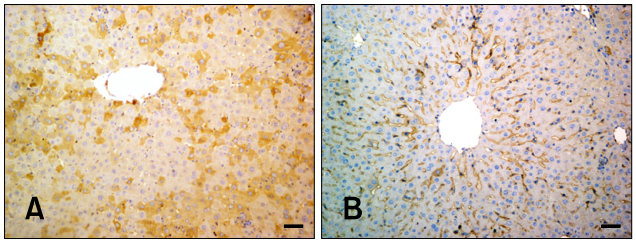

Fig. 4. VEGF expression in hepatocytes from the experimental and control groups. (A) Cytoplasmic VEGF immunolabeling (Group 4B). (B) VEGF staining shown in panel B was significantly decreased compared that observed in panel A (Group 6C). Scale bars = 44 μm.

VEGF

Hepatocytes from the control group and mice treated with silymarin alone showed weak, diffuse cytoplasmic staining limited to the periacinar and periportal areas. Immunostaining of the hepatocytes were elevated significantly upon FB_1 administration in Groups 3 and 4 (Fig. 4A). Silymarin treatment caused a significant decrease in VEGF expression, particularly in Group 6 (Fig. 4B; $p < 0.0001$).

Discussion

In mice, apoptosis was found in the liver after short-term treatment with FB_1 [8]. FB_1-induced apoptosis altered cell proliferation. Altered signal transduction processes are believed to be linked to fumonisin-induced changes in the biosynthesis of sphingoid bases, sphingoid base metabolites, ceramide, and more complex sphingolipids [18]. The ability of FB_1 to induce apoptosis appears to be important for the toxic effects of this reagent. In the present study, silymarin administration significantly attenuated FB_1-induced apoptosis in Group 5.

The cellular effects of fumonisins consist of a mixture of apoptosis and regenerative proliferation [16]. Therefore, the effect of FB_1 treatment on hepatocyte proliferation rates has also been evaluated by measuring PCNA and Ki-67 expression. In the present study, apoptosis and PCNA expression levels were elevated in FB_1-treated Groups 3 and 4, similar to previous findings [16].

It has been reported that silymarin significantly augments PCNA expression and diminishes the number of apoptotic hepatocytes in the liver of mice exposed to FB_1 [10]. It was also suggested that silymarin increases cellular regeneration while decreasing cellular damage [10]. However, in our study silymarin significantly reduced the number of apoptotic hepatocytes in both Groups 5 and 6 but cell proliferation rates measured by PCNA expression were not significantly altered. This difference may possibly be due to the limited days of FB_1 treatment (2.25 mg/kg for 3 days) and 750 mg/kg silymarin administration in the previous study compared to our higher repeated seven doses of FB_1 and lower dose of silymarin (100 mg/kg). On the other hand, Ki-67 expression was elevated in Group 5 compared to Group 3. This increase suggests that silymarin positively affects the regeneration of damaged hepatocytes while reducing cellular damage when co-administered with FB_1.

Cell signalling factors including TNFα play significant roles in FB_1-induced liver toxicity [4,5]. It has been reported that FB_1 treatment elevates the number of peripheral leukocytes and leukocytes abrogated by pre-treatment with anti-TNFα antibody that reduces the toxic effects of FB_1 [9]. Silymarin protects the liver from hepatotoxin-induced liver damage by blocking intrahepatic nuclear factor kappa B (NF-κB) activation and consequently inhibiting intrahepatic TNFα expression [21]. In the present study, silymarin effectively prevented TNFα production induced by FB_1 application similar to study performed by Schümann *et al*. [21].

Another factor that reduces fumonisin toxicity involves the inhibition of caspases that belongs to the family of TNFα cellular signal mediators [6]. In the present study, caspase-8, an intracellular molecule involved in the regulation of apoptosis, was evaluated. FB_1 application induced the intrahepatic expression of caspase-8 while silymarin administration significantly diminished the elevated caspase-8 levels. In a recent investigation, silibinin (a major active constituent of silymarin) was found to inhibit UV-induced HaCaT cell apoptosis through the caspase-8 pathway [15].

Gal-3 is present only in Kupffer cells and not hepatocytes in the mouse liver [14]. Despite its low level in normal liver tissues, Gal-3 expression increases significantly during preneoplastic changes, intrahepatic cholangiocarcinomas, hepatocellular cancers, and cirrhosis [11,22]. In the current study and a previous investigation [14], Gal-3 expression was detected only in Kupffer cells in the livers of the control and mice treated with silymarin alone. Increased diffuse cytoplasmic signals specific for Gal-3 were detected in hepatocytes from Groups 3 and 4. Gal-3 identified in rat hepatocytes damaged by CCl_4 indicates that Gal-3 promotes the repair or survival of the injured hepatocytes [28]. In the same study, the authors also postulated that simultaneous expression of PCNA and Gal-3 in both the nucleus and cytoplasm demonstrates that the hepatocytes are quiescent and cellular damage is being repaired [28]. In the present study, silymarin reduced the elevated Gal-3 expression induced by FB_1. Taking all our findings into consideration, Gal-3 may be involved in the defense systems that confer protection against exogenous toxins. Additionally, silymarin also reduces the effects of toxins such as FB_1.

Results from our investigation showed that FB_1 administration elevates VEGF and FGF-2 expression in mouse liver. FGF-2 and VEGF act synergistically during

angiogenesis [1]. FGF-2 is an effective mitogen that induces the migration of endothelial cells and fibroblasts [2]. For this reason, it was suggested that angiogenesis is stimulated primarily by VEGF while FGF-2 contributes to the maintenance of angiogenesis [20]. We observed a prominent up-regulation of VEGF expression in particular periportal and periacinar regions of the liver from mice exposed to FB_1. These findings are consistent with those from previous reports indicating that VEGF expression is induced following CCl_4 and acetaminophen administration [7,13] and ischemia/reperfusion injury [25]. Taniguchi *et al*. [24] showed that partial hepatectomy also increases VEGF expression and contributes to liver regeneration in rats. Furthermore, VEGF expression is up-regulated during hypoxia-initiated angiogenesis [23]. It was suggested that VEGF is a transducer that conveys signals between endothelial and epithelial/mesenchymal cells, and activates angiogenesis [13].

In the present study, we observed increased VEGF labeling in the hepatocytes located in close proximity to the veins. It could be speculated that partial hypoxia occurred as a result of damage due to FB_1 toxicity and was responsible for the VEGF up-regulation we observed. To facilitate sufficient blood flow, hepatocytes could produce VEGF followed by sinusoidal reparation and hepatocellular proliferation [24]. It is interesting to note that the use of a VEGF antagonist that prevents ischemia/reperfusion injury protects mouse livers [25]. This beneficial effect involves the up-regulated expression of antioxidant/anti-apoptotic cytoprotective genes similar to that of the silymarin used in this study [25]. Furthermore, silymarin treatment was found to diminish VEGF mRNA levels in the fibrotic livers of bile duct-ligated rats [12]. The anti-angiogenic effect of silymarin is associated with increased VEGF receptor gene expression (Flt-1) [29]. Data from the present study suggest that silymarin neutralizes *in vivo* VEGF protein expression during the recovery from FB_1 toxicity. Inhibition of VEGF signalling with silymarin possibly delays hepatocyte regeneration. This effect was partly associated with reduced expression of caspase-8.

In conclusion, FB_1-induced hepatocyte damage was significantly reversed by co-treatment with silymarin in BALB/c mice. The hepatoprotective effect of silymarin may be attributed to its antioxidant activity. Silymarin is widely available as an herbal supplement and could be used as a protective agent in both humans and animals exposed to fumonisin-contaminated feed.

Acknowledgments

This study was funded by the Scientific and Technological Research Council of Turkey (TUBITAK-TOVAG; Project No. 106 O 197), Turkey. We thank Dr. Ronald Riley (Toxicology and Mycotoxin Research Unit, United States Department of Agriculture-Agricultural Research Service, USA) for generously supplying FB_1.

References

1. **Ankoma-Sey V, Matli M, Chang KB, Lalazar A, Donner DB, Wong L, Warren RS, Friedman SL.** Coordinated induction of VEGF receptors in mesenchymal cell types during rat hepatic wound healing. Oncogene 1998, **17**, 115-121.
2. **Basilico C, Moscatelli D.** The FGF family of growth factors and oncogenes. Adv Cancer Res 1992, **59**, 115-165.
3. **Bhandari N, He Q, Sharma RP.** Gender-related differences in subacute fumonisin B1 hepatotoxicity in BALB/c mice. Toxicology 2001, **165**, 195-204.
4. **Bhandari N, Sharma RP.** Fumonisin B1-induced alterations in cytokine expression and apoptosis signaling genes in mouse liver and kidney after an acute exposure. Toxicology 2002, **172**, 81-92.
5. **Bhandari N, Sharma RP.** Modulation of selected cell signaling genes in mouse liver by fumonisin B1. Chem Biol Interact 2002, **139**, 317-331.
6. **Ciacci-Zanella JR, Jones C.** Fumonisin B1, a mycotoxin contaminant of cereal grains and inducer of apoptosis via the tumor necrosis factor pathway and caspase activation. Food Chem Toxicol 1999, **37**, 703-712.
7. **Donahower B, Mc Cullough SS, Kurten R, Lamps LW, Simpson P, Hinson JA, James LP.** Vascular endothelial growth factor and hepatocyte regeneration in acetaminophen toxicity. Am J Physiol Gastrointest Liver Physiol 2006, **291**, G102-109.
8. **Dragan YP, Bidlack WR, Cohen SM, Goldsworthy TL, Hard GC, Howard PC, Riley RT, Voss KA.** Implications of apoptosis for toxicity, carcinogenicity, and risk assessment: fumonisin B1 as an example. Toxicol Sci 2001, **61**, 6-17.
9. **Dugyala RR, Sharma RP, Tsunoda M, Riley RT.** Tumor necrosis factor-α as a contributor in fumonisin B1-toxicity. J Pharmacol Exp Ther 1998, **285**, 317-324.
10. **He Q, Kim J, Sharma RP.** Silymarin protects against liver damage in BALB/c mice exposed to fumonisin B1 despite increasing accumulation of free sphingoid bases. Toxicol Sci 2004, **80**, 335-342.
11. **Hsu DK, Dowling CA, Jeng KCG, Chen JT, Yang RY, Liu FT.** Galectin-3 expression is induced in cirrhotic liver and hepatocellular carcinoma. Int J Cancer 1999, **81**, 519-526.
12. **Hsu YC, Chiu YT, Lee CY, Wu CF, Huang YT.** Anti-fibrotic effects of tetrandrine on bile-duct ligated rats. Can J Physiol Pharmacol 2006, **84**, 967-976.
13. **Ishikawa K, Mochida S, Mashiba S, Inao M, Matsui A, Ikeda H, Ohno A, Shibuya M, Fujiwara K.** Expressions of vascular endothelial growth factor in nonparenchymal as well as parenchymal cells in rat liver after necrosis. Biochem Biophys Res Commun 1999, **254**, 587-593.
14. **Kim H, Lee J, Hyun JW, Park JW, Joo H, Shin T.** Expression and immunohistochemical localization of

galectin-3 in various mouse tissues. Cell Biol Int 2007, **31**, 655-662.

15. **Li LH, Wu LJ, Tashiro S, Onodera S, Uchiumi F, Ikejima T.** Silibinin prevents UV-induced HaCaT cell apoptosis partly through inhibition of caspase-8 pathway. Biol Pharm Bull 2006, **29**, 1096-1101.
16. **Lim CW, Parker HM, Vesonder RF, Haschek WM.** Intravenous fumonisin B1 induces cell proliferation and apoptosis in the rat. Nat Toxins 1996, **4**, 34-41.
17. **Liu FT, Patterson RJ, Wang JL.** Intracellular functions of galectins. Biochim Biophys Acta 2002, **1572**, 263-273.
18. **Merrill AH Jr., Schmelz EM, Dillehay DL, Spiegel S, Shayman JA, Schroeder JJ, Riley RT, Voss KA, Wang E.** Sphingolipids-the enigmatic lipid class: biochemistry, physiology, and pathophysiology. Toxicol Appl Pharmacol 1997, **142**, 208-225.
19. **Rastogi R, Srivastava AK, Srivastava M, Rastogi AK.** Hepatocurative effect of picroliv and silymarin against aflatoxin B1 induced hepatotoxicity in rats. Planta Med 2000, **66**, 709-713.
20. **Rosmorduc O, Wendum D, Corpechot C, Galy B, Sebbagh N, Raleigh J, Housset C, Poupon R.** Hepatocellular hypoxia-induced vascular endothelial growth factor expression and angiogenesis in experimental biliary cirrhosis. Am J Pathol 1999, **155**, 1065-1073.
21. **Schümann J, Prockl J, Kiemer AK, Vollmar AM, Bang R, Tiegs G.** Silibinin protects mice from T cell-dependent liver injury. J Hepatol 2003, **39**, 333-340.
22. **Shimonishi T, Miyazaki K, Kono N, Sabit H, Tuneyama K, Harada K, Hirabayashi J, Kasai K, Nakanuma Y.** Expression of endogenous galectin-1 and galectin-3 in intrahepatic cholangiocarcinoma. Hum Pathol 2001, **32**, 302-310.
23. **Shweiki D, Itin A, Soffer D, Keshet E.** Vascular endothelial growth factor induced by hypoxia may mediate hypoxia-initiated angiogenesis. Nature 1992, **359**, 843-845.
24. **Taniguchi E, Sakisaka S, Matsuo K, Tanikawa K, Sata M.** Expression and role of vascular endothelial growth factor in liver regeneration after partial hepatectomy in rats. J Histochem Cytochem 2001, **49**, 121-129.
25. **Tsuchihashi S, Ke B, Kaldas F, Flynn E, Busuttil RW, Briscoe DM, Kupiec-Weglinski JW.** Vascular endothelial growth factor antagonist modulates leukocyte trafficking and protects mouse livers against ischemia/reperfusion injury. Am J Pathol 2006, **168**, 695-705.
26. **Voss KA, Riley RT, Bacon CW, Chamberlain WJ, Norred WP.** Subchronic toxic effects of Fusarium moniliforme and fumonisin B1 in rats and mice. Nat Toxins 1996, **4**, 16-23.
27. **WHO IPCS.** Fumonisin B1. Environmental Health Criteria 219. pp. 1-150, World Health Organization, **Geneva**, 2000.
28. **Yamazaki K, Kawai A, Kawaguchi M, Hibino Y, Li F, Sasahara M, Tsukada K, Hiraga K.** Simultaneous induction of galectin-3 phosphorylated on tyrosine residue, p21WAF1/Cip1/Sdi1, and the proliferating cell nuclear antigen at a distinctive period of repair of hepatocytes injured by CCl4. Biochem Biophys Res Commun 2001, **280**, 1077-1084.
29. **Yang SH, Lin JK, Huang CJ, Chen WS, Li SY, Chiu JH.** Silibinin inhibits angiogenesis via Flt-1, but not KDR, receptor up-regulation. J Surg Res 2005, **128**, 140-146.
30. **Zi X, Mukhtar H, Agarwal R.** Novel cancer chemopreventive effects of a flavonoid antioxidant silymarin: inhibition of m RNA expression of an endogenous tumor promoter TNFα. Biochem Biophys Res Commun 1997, **239**, 334-339.